Egyptian Journal of Petroleum (2015) **24**, 333–341

HOSTED BY

ELSEVIER

Egyptian Petroleum Research Institute

Egyptian Journal of Petroleum

www.elsevier.com/locate/egyjp
www.sciencedirect.com

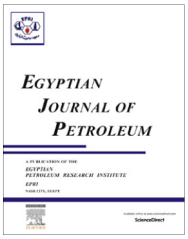

FULL LENGTH ARTICLE

Effect of solution pH on the electrochemical behaviour of AISI 304 austenitic and AISI 430 ferritic stainless steels in concentrated acidic media

A. Fattah-alhosseini *, **S. Vafaeian**

Department of Materials Engineering, Bu-Ali Sina University, Hamedan 65178-38695, Iran

Received 15 May 2014; accepted 24 June 2014
Available online 22 July 2015

KEYWORDS

Stainless steel;
pH;
Mott–Schottky;
Donor density;
Acceptor density

Abstract In this study, the effect of solution pH on the electrochemical behaviour of AISI 304 austenitic and AISI 430 ferritic stainless steels at open circuit potential (OCP) in concentrated acidic solutions was studied. Polarization curves showed that the corrosion current density of both stainless steels increased with decreasing pH. Mott–Schottky analysis revealed that passive films formed on AISI 304 and AISI 430 stainless steels behave as *n*-type and *p*-type semiconductors and the donor and acceptor densities increased with decreasing pH. Electrochemical impedance spectroscopy (EIS) results showed that the reciprocal capacitance of the passive film is directly proportional to its thickness which decreases with decreasing pH. Thus for both austenitic and ferritic stainless steels in acidic solutions, increasing the solution pH offers better conditions for forming passive films with higher protection behaviour, due to the growth of much thicker and less defective films.

1. Introduction

Stainless steels are used in applications where high corrosion resistance is required. These alloys are the most common multi-component construction materials used by chemical and petrochemical industries. The corrosion resistance of stainless steels is due to the presence of passive films (iron and chromium oxide films with semiconducting behaviour). In the last decade, a lot of research of the electronic properties of passive films formed on stainless steels has given an important contribution to the understanding of the corrosion behaviour of these alloys. Generally, the film composition varies with the solution pH used for film formation and this is expected to affect the semiconducting properties of the passive film [1,2].

In practice, an increase or decrease of solution pH has significant effects on the corrosion behaviour of stainless steels. The main effect of an increasing pH on film formation is a thickening of the passive film, basically because iron oxides are more stable in alkaline solutions. Conversely, in acid solutions a chromium-rich oxide film is formed due to slower dissolution of chromium oxide when compared to iron oxide [3,4]. It is found that nitric acid concentration has a significant

* Corresponding author. Fax: +98 811 8257400.
E-mail address: a.fattah@basu.ac.ir (A. Fattah-alhosseini).

Peer review under responsibility of Egyptian Petroleum Research Institute.

http://dx.doi.org/10.1016/j.ejpe.2015.07.016

Table 1 Chemical compositions of AISI 304 austenitic and AISI 430 ferritic stainless steels.

	Cr	Ni	Mo	Mn	Si	C	P	Cu	N	Co	Fe
AISI 304/wt%	18.62	8.2	0.04	1.19	0.60	0.05	0.002	0.20	–	0.15	Bal
AISI 430/wt%	16.50	0.13	0.02	0.53	0.50	0.05	0.025	0.07	0.06	0.02	Bal

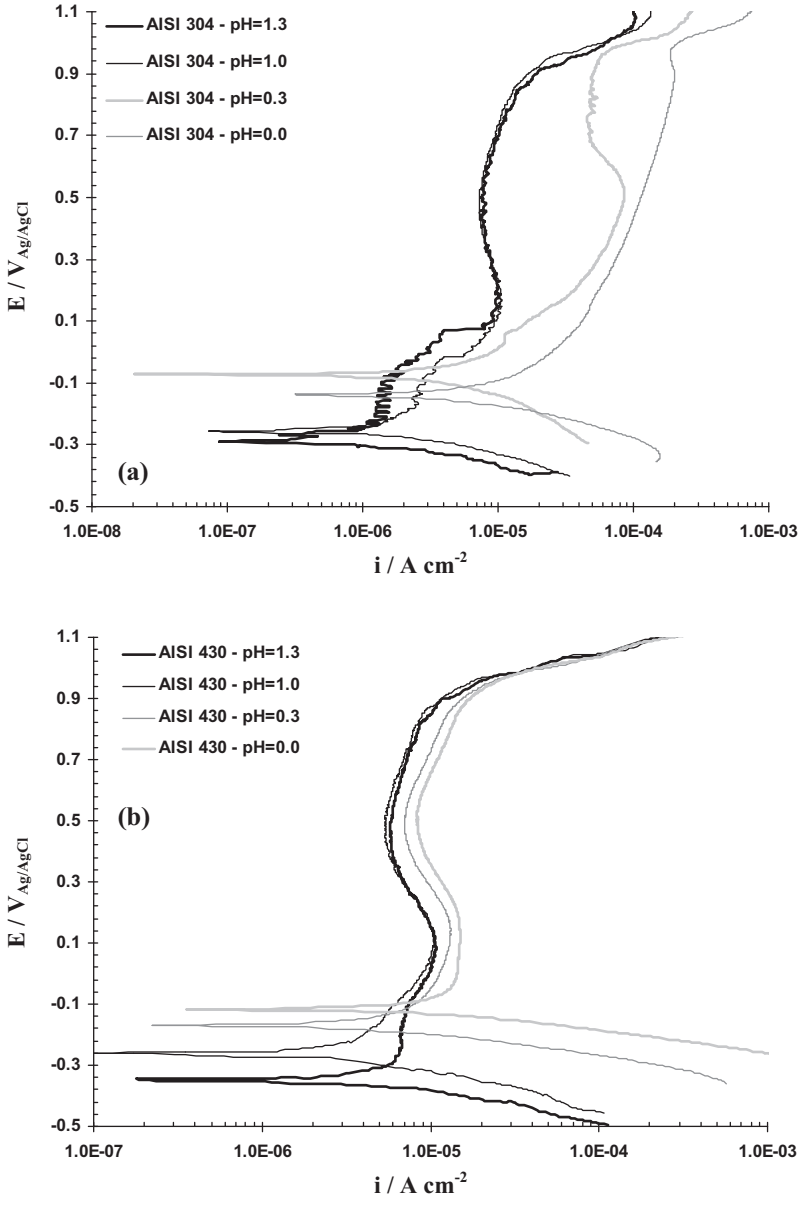

Figure 1 Potentiodynamic polarization curves of AISI 304 and AISI 430 stainless steels in HNO_3 solutions with pH varying from 1.3 to 0.0.

effect on the corrosion behaviour of stainless steel [5]. In the other study, the anodic polarization curves showed no significant changes in corrosion potential even with an increase in nitric acid concentration in the presence of oxidizing ions [6]. For austenitic stainless steel in nitric acid solutions, it is found [7] that the passive film consists of platelet-like structures at lower concentrations of nitric acid. This study also showed that at higher concentrations of nitric acid, the platelet-like structures disappear. Also, it is found that the variation in passive film morphology (For austenitic stainless steel) occurs depending upon the concentration and time of immersion [8].

According to the Point Defect Model (PDM) [9–11], the growth of the passive film involves the migration of these point defects under the influence of the electrostatic field in the film. Thus, the key parameters in determining the transport of point defects and hence the kinetics of film growth is the density and

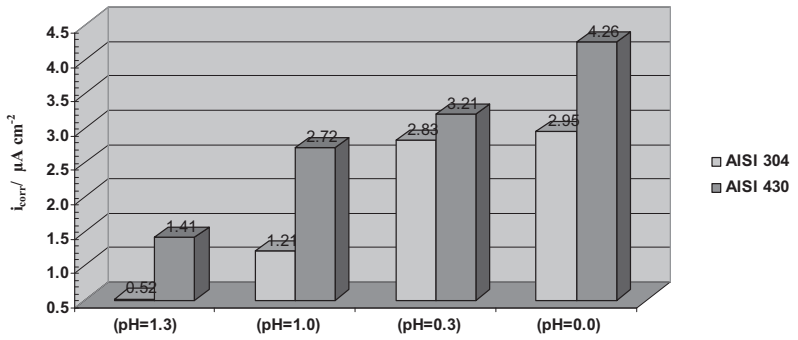

Figure 2 Effect of solution pH on the corrosion current density of AISI 304 and AISI 430 stainless steel.

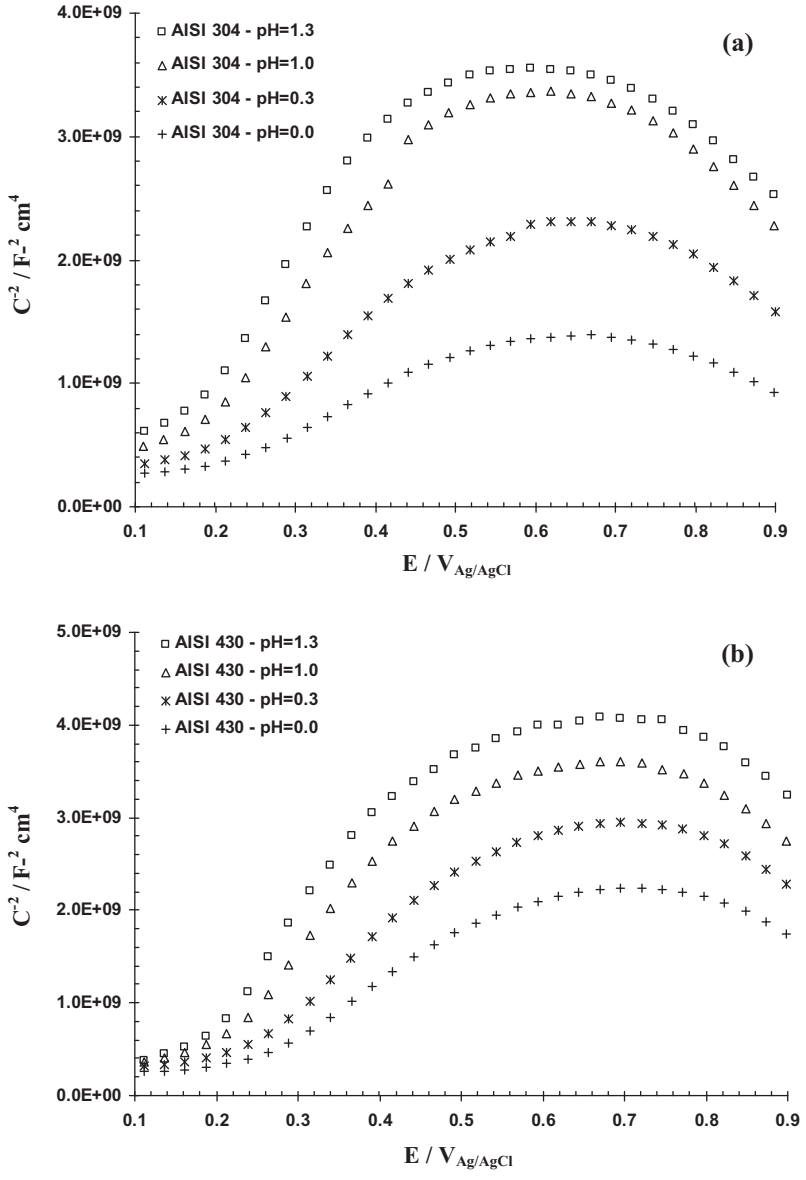

Figure 3 Mott–Schottky plots of (a) AISI 304 and (b) AISI 430 stainless steels in HNO_3 solutions with pH varying from 1.3 to 0.0.

the diffusivity of the defects in the film. In the last decade, by employing the Mott–Schottky analysis in conjunction with the PDM, the point defect density and diffusivity of some metals and alloys have been determined [9–11].

However, there is still lack of study on the effect of solution pH on the diffusivities of point defects in the passive film formed on stainless steels. In this work, the Mott–Schottky analysis of AISI 304 austenitic and AISI 430 ferritic stainless

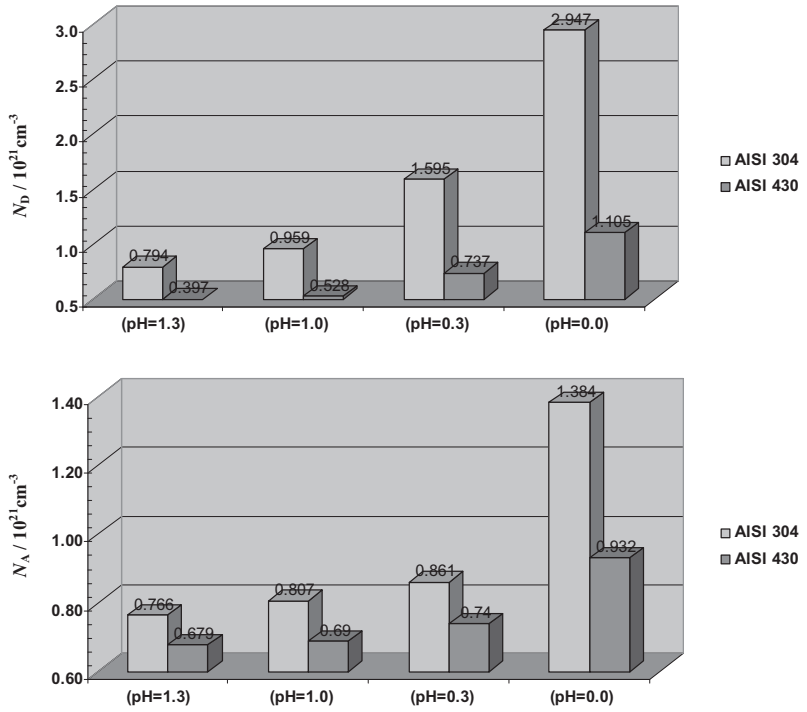

Figure 4 Effect of solution pH on the (a) donor and (b) acceptor density of the passive films formed on AISI 304 and AISI 430 stainless steels.

steels in HNO_3 solutions was performed and the defect concentrations were calculated as a function of pH solution. The relationship between the donor and acceptor density and pH solution is discussed in order to understand the property of the passivation of AISI 304 austenitic and AISI 430 ferritic stainless steels.

2. Experimental procedures

The chemical composition of AISI 304 austenitic and AISI 430 ferritic stainless steels used in the present investigation is shown in Table 1. All samples were ground to 1200 grit and cleaned by distilled water prior to tests. Aerated acidic solutions (without purging oxygen or any gas) with HNO_3 and distilled water were prepared at different pH (1.3, 1.0, 0.3, and 0.0). All electrochemical measurements were performed in a conventional three-electrode flat cell. The counter electrode was a Pt plate, and all potentials were measured against Ag/AgCl in saturated KCl. All electrochemical measurements were obtained using METROHM AUTOLAB potentiostat/galvanostat controlled by a personal computer. Prior to all electrochemical measurements, working electrodes were immersed at OCP in solutions to form a steady-state passive film. Potentiodynamic polarization curves were measured potentiodynamically at a scan rate of 1 mV s^{-1} starting from −0.25 V (vs. E_{corr}) to 1.1 V. The impedance spectra were measured in a frequency range of 100 kHz–10 mHz at an AC amplitude of 10 mV (rms). For the EIS data modelling and curve-fitting method, the NOVA impedance software was used. Mott–Schottky analysis was carried out on the passive films at a frequency of 1 kHz using a 10 mV ac signal and a step potential of 25 mV, in the cathodic direction.

3. Results and discussion

3.1. Potentiodynamic polarization measurements

Fig. 1 shows the potentiodynamic polarization curves of AISI 304 austenitic and AISI 430 ferritic stainless steels in HNO_3 solutions with pH varying from 1.3 to 0.0. By comparing the polarization curves of both stainless steels in different pH solutions, the current density was found to increase with potential during the early stage of passivation and no obvious current peak was observed. Also, all curves exhibit similar features, with a passive potential range extending from the corrosion potential to the onset of transpassivity.

Tafel extrapolation method is widely used for the measurement of the corrosion rate of alloys. Indeed, the corrosion current density (i_{corr}) was calculated by Tafel extrapolation of the linear part of the cathodic branch back to the mixed potential of zero net current (E_{corr}) with an accuracy of more than 95% for the points more negative to E_{corr} by 50 mV [12–14].

Fig. 2 shows the effect of solution pH on the corrosion current density of AISI 304 and AISI 430 stainless steels. It is evident from this figure that the corrosion current density increased with decreasing pH.

3.2. Mott–Schottky analysis

The outer layer of passive films contains the space charge layer and sustains a potential drop across the film. The charge

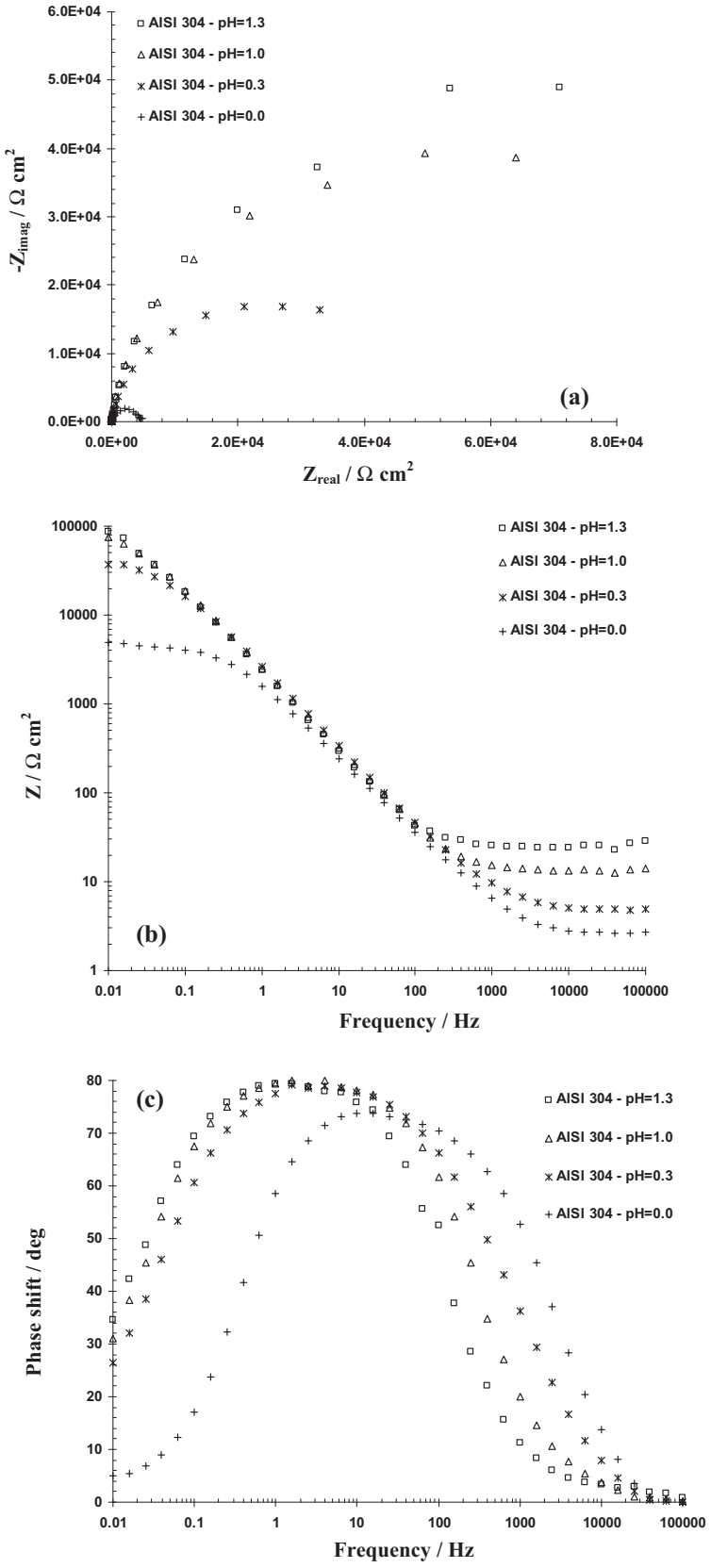

Figure 5 (a) Nyquist, (b) Bode and (c) Bode-phase plots of AISI 304 stainless steels in HNO_3 solutions with pH varying from 1.3 to 0.0.

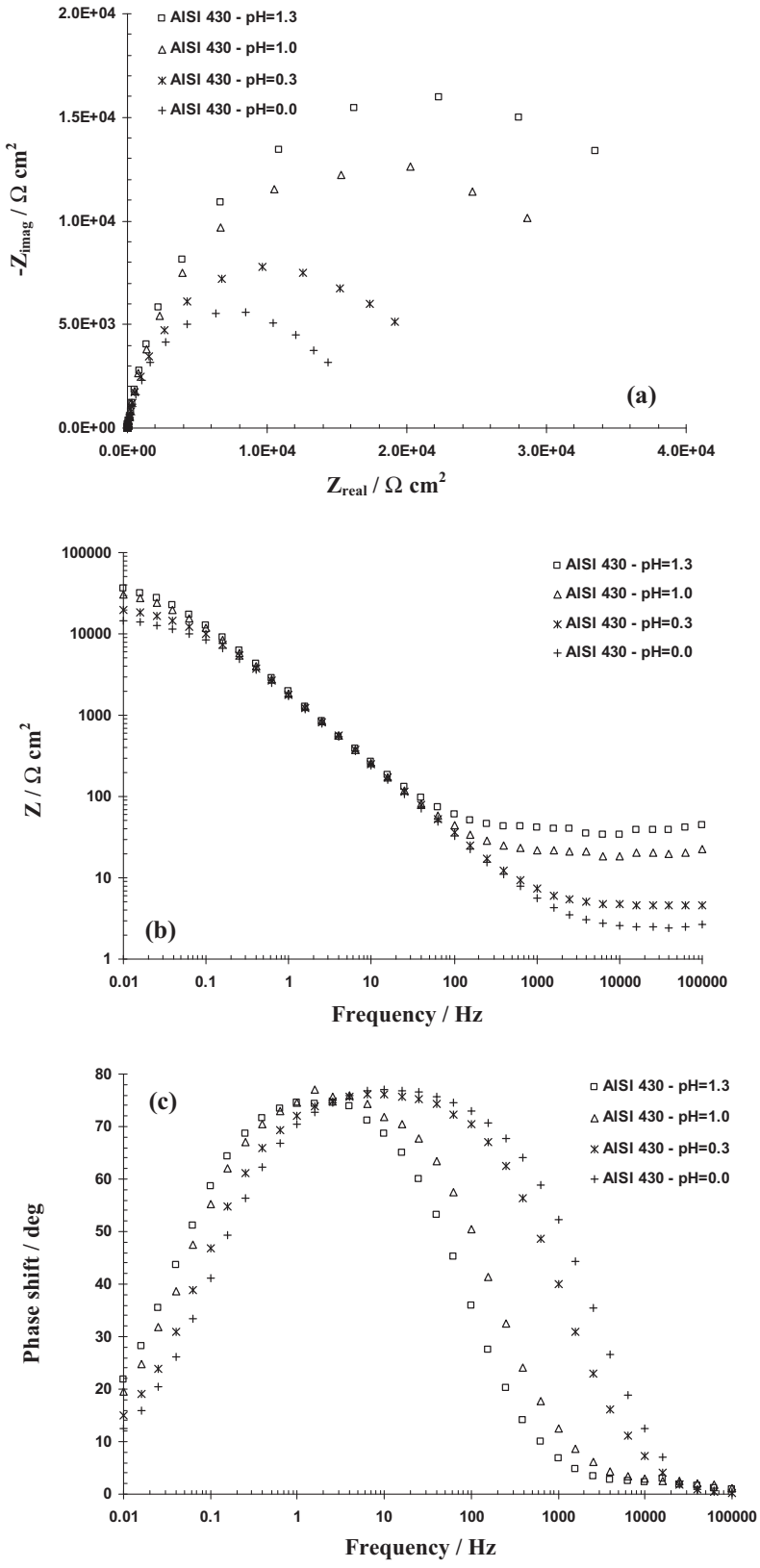

Figure 6 (a) Nyquist, (b) Bode and (c) Bode-phase plots of AISI 430 stainless steels in HNO_3 solutions with pH varying from 1.3 to 0.0.

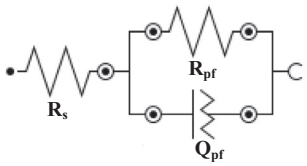

Figure 7 The best equivalent circuit tested to model the experimental EIS data with one time constant.

distribution at the semiconductor/solution is usually determined based on Mott–Schottky relationship by measuring electrode capacitance C, as a function of electrode potential E [15–17]:

$$\frac{1}{C^2} = \frac{2}{\varepsilon\varepsilon_0 e N_D}\left(E - E_{FB} - \frac{kT}{e}\right) \quad \text{for } n\text{-type semiconductor} \tag{1}$$

$$\frac{1}{C^2} = -\frac{2}{\varepsilon\varepsilon_0 e N_A}\left(E - E_{FB} - \frac{kT}{e}\right) \quad \text{for } p\text{-type semiconductor} \tag{2}$$

where e is the electron charge (-1.602×10^{-19} C), N_D is the donor density for n-type semiconductor (cm^{-3}), N_A is the acceptor density for p-type semiconductor (cm^{-3}), ε is the dielectric constant of the passive film (usually taken as 15.6 [15–17]), ε_0 is the vacuum permittivity (8.854×10^{-14} F cm^{-1}), k is the Boltzmann constant, T is the absolute temperature and E_{FB} is the flat band potential. Flat band potential can be determined from the extrapolation of the linear portion to $C^{-2} = 0$.

Fig. 3 shows the Mott–Schottky plots of AISI 304 austenitic and AISI 430 ferritic stainless steels in HNO_3 solutions with pH varying from 1.3 to 0.0. It should be noted that for both stainless steels, C^{-2} clearly decreases with decreasing pH. In this Figure, the positive and negative slopes in the main passive region are attributed to n-type and p-type behaviours, respectively. According to Eqs. (1) and (2), donor and acceptor densities have been determined from the positive and negative slopes in the main passive region.

Fig. 4(a) and (b) shows the calculated donor and acceptor densities for the passive films formed on AISI 304 austenitic and AISI 430 ferritic stainless steels in HNO_3 solutions with pH varying from 1.3 to 0.0. The orders of magnitude are around 10^{21} cm^{-3} and are comparable to those reported in other studies [18]. According to Fig. 4(a) and (b), the donor and acceptor densities increase with decreasing pH. Based on PDM [10], the flux of oxygen vacancy and/or cation interstitials through the passive film is essential to the film growth process. In this concept, the dominant point defects in the passive film are considered to be oxygen vacancies and/or cation interstitials acting as electron donors. Also, chromium vacancies or excess oxygen can be related to this p-type semiconductor behaviour of chromium oxide in passive films [19,20].

3.3. EIS measurements

The EIS response of AISI 304 austenitic and AISI 430 ferritic stainless steels in HNO_3 solutions with pH varying from 1.3 to 0.0 was performed and results are presented as Nyquist and Bode plots in Figs. 5 and 6, respectively. For both stainless steels, the Nyquist and Bode plots show a resistive behaviour at high frequencies, but in the middle to low frequency ranges

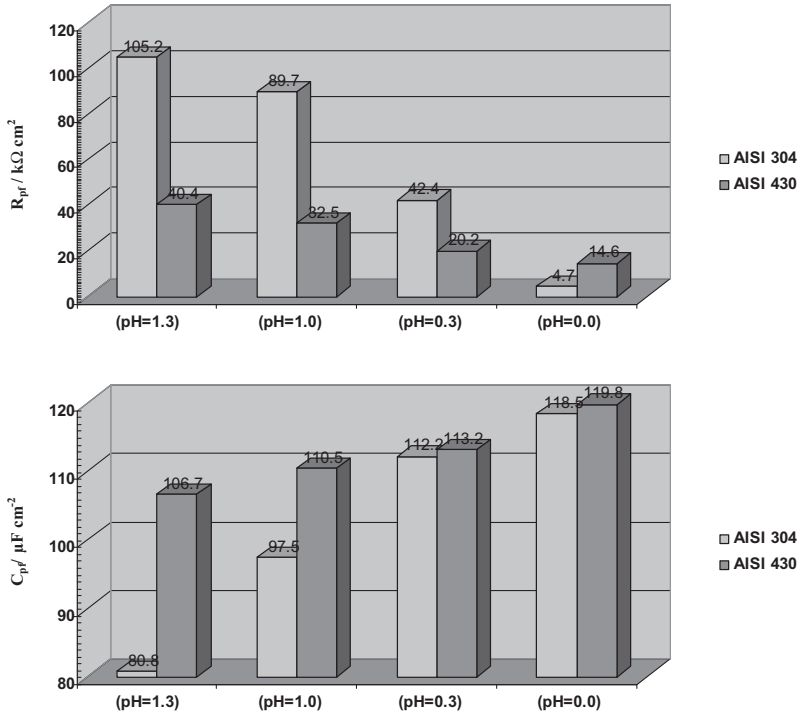

Figure 8 Effect of solution pH on the (a) passive film resistance and (b) passive film capacitance of AISI 304 and AISI 430 stainless steels in HNO_3 solutions.

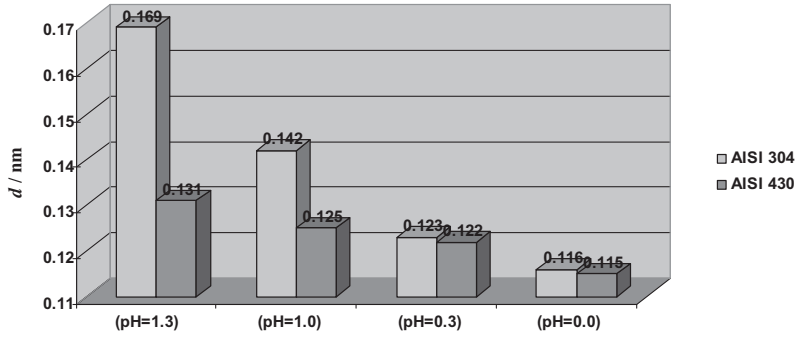

Figure 9 Effect of solution pH on the passive film thickness of AISI 304 and AISI 430 stainless steels in HNO_3 solutions.

there was a marked capacitive response. The Bode-phase curves show one time constant (only one maximum phase lag at the middle frequency range). The phase angle values remained very close to 80°. This evolution revealed the formation and growth of a passive film. Also, there was a decrease of the low frequency impedance with decreasing pH.

Based on these results, the equivalent circuit shown in Fig. 7 was used to simulate the measured impedance data of AISI 304 austenitic and AISI 430 ferritic stainless steels in HNO_3 solutions with pH varying from 1.3 to 0.0. This equivalent circuit is composed of: R_s – solution resistance; Q_{pf} – constant phase element corresponding to the capacitance of the passive film; R_{pf} – resistance of the passive film. This equivalent circuit was composed of a one time constant as proposed by Pardo et al. [21] to describe the behaviour of AISI 304 and 316 stainless steels in H_2SO_4 solutions. The impedance of the constant phase element is presented using the Eq. (3):

$$Z_Q = [C(j\omega)^n]^{-1} \tag{3}$$

where n is associated with the roughness of the electrode surface [21]. Fig. 8 shows the effect of solution pH on the passive film resistance and capacitance of AISI 304 and AISI 430 stainless steels. As can be seen in Fig. 8, for both stainless steels, passive film resistance decreases with decreasing pH while passive film capacitance increases. According to the equivalent circuit shown in Fig. 7, the passive film thickness (d) can be calculated using the Eq. (4) [22]:

$$d = \frac{\varepsilon\varepsilon_0 A}{C} \tag{4}$$

where C is the total capacitance of the passive film, and A the area in cm^2. Generally, a change in the total capacitance of the passive film can be used as an indicator for change in the passive film thickness. Therefore, the reciprocal capacitance of the passive film ($1/C$) is proportional to its thickness which decreases with decreasing pH. Fig. 9 shows the effect of solution pH on the passive film thickness of AISI 304 and AISI 430 stainless steels. As can be seen in Fig. 9, for both stainless steels, passive film thickness decreases with decreasing pH. These values of the thickness are considered to be eminently realistic [24]. It is clear that increasing the solution pH gives better conditions for forming the passive films with higher protection behaviour, due to the growth of much thicker and less defective passive films [23].

4. Conclusions

(1) Potentiodynamic polarization curves showed that the corrosion current density of both AISI 304 and AISI 430 stainless steels increased with decreasing pH.
(2) Mott–Schottky analysis revealed that passive films formed on AISI 304 and AISI 430 stainless steels behave as n-type and p-type semiconductors and the donor and acceptor densities increased with decreasing pH.
(3) EIS results showed that the reciprocal capacitance of the passive film decreases with decreasing pH.
(4) Also, EIS results showed that increasing the solution pH offers better conditions for forming passive films with higher protection behaviour, due to the growth of much thicker and less defective films.

References

[1] Y.Y. Chen, Y.M. Liou, H.C. Shih, Mater. Sci. Eng., A 407 (2005) 114–126.
[2] A.A. Hermas, M.S. Morad, Corros. Sci. 50 (2008) 2710–2717.
[3] M.V. Cardoso, S.T. Amaral, E.M.A. Martini, Corros. Sci. 50 (2008) 2429–2436.
[4] M.J. Carmezim, A.M. Simões, M.F. Montemor, M. Da Cunha Belo, Corros. Sci. 47 (2005) 581–589.
[5] S. Ningshen, U.K. Mudali, G. Amarendra, B. Raj, Corros. Sci. 53 (2011) 64–70.
[6] S. Ningshen, U.K. Mudali, G. Amarendra, B. Raj, Corros. Sci. 51 (2009) 322–329.
[7] N. Padhy, S. Ningshen, U.K. Mudali, G. Amarendra, B. Raj, Scripta Mater. 62 (2010) 45–48.
[8] N. Padhy, S. Ningshen, U.K. Mudali, G. Amarendra, B. Raj, Appl. Surf. Sci. 257 (2011) 5088–5097.
[9] E. Sikora, D.D. Macdonald, J. Electrochem. Soc. 147 (2000) 4087–4092.
[10] D.D. Macdonald, J. Nucl. Mater. 379 (2008) 24–32.
[11] A. Fattah-alhosseini, M.A. Golozar, A. Saatchi, K. Raeissi, Corros. Sci. 52 (2010) 205–209.
[12] M.A. Amin, G.A.M. Mersal, Q. Mohsen, Arab. J. Chem. 4 (2011) 223–229.
[13] G.T. Burstein, Corros. Sci. 47 (2005) 2858–2865.
[14] S.J. Lee, C.H. Huang, Y.P. Chen, J. Mater. Process. Technol. 140 (2003) 688–694.
[15] Y.F. Cheng, C. Yang, J.L. Luo, Thin Solid Films 416 (2002) 169–173.
[16] N. Li, Y. Li, S. Wang, F. Wang, Electrochim. Acta 52 (2006) 760–765.

[17] C. Escrivà-Cerdán, E. Blasco-Tamarit, D.M. García-García, J. García-Antóna, A. Guenbour, Electrochim. Acta 80 (2012) 248–256.
[18] E.E. Oguzie, J. Li, Y. Liu, D. Chen, Y. Li, K. Yang, F. Wang, Electrochim. Acta 55 (2010) 5028–5035.
[19] F. Gaben, B. Vuillemin, R. Oltra, J. Electrochem. Soc. 151 (2004) B595–B604.
[20] S. Virtanen, P. Schmuki, H. Bohni, P. Vuoristo, T. Mantyla, J. Electrochem. Soc. 142 (1995) 3067–3072.
[21] A. Pardo, M.C. Merino, M. Carboneras, F. Viejo, R. Arrabal, J. Munoz, Corros. Sci. 48 (2006) 1075–1081.
[22] J. Chen, J.Q. Wang, E.H. Han, J.H. Dong, W. Ke, Corros. Sci. 50 (2008) 1292–1305.
[23] F.E.T. Heakal, A.M. Fekry, M.A.E.B. Jibril, Corros. Sci. 53 (2011) 1174–1185.
[24] C.O.A. Olsson, D. Landolt, Electrochim. Acta 48 (2003) 1093–1104.